

RESEARCH ARTICLE

Formulation, Characterization, Optimization, and *In-vitro* Evaluation of Rosuvastatin as Nanofiber

Ihsan A Mohammed¹, Fatima J Al-Gawhari²

¹Ministry of Health and Environment, Babylon Health Directorate, Babylon, Iraq

²Department of Pharmaceutics, University of Baghdad, College of Pharmacy, Iraq.

Received: 07th July, 2023; Revised: 29th September, 2023; Accepted: 19th October, 2023; Available Online: 25th December, 2023

ABSTRACT

Bioavailability is the objective for an optimum formulation. The target of the analysis is to maximize both the fluidity and disintegration profile of class II weakly compounds that are water-soluble. Anti-dyslipidemia drug rosuvastatin calcium (RC) (bioavailability 20%) through formulating as nanofibers (NFs) using electrospinning (ES) technology. Twenty formulas were prepared, and different polymers and polymer combinations with various concentrations were used such as polyethylene oxide (PEO) polyvinyl pyrrolidone (PVPK-30), and hydroxypropyl methylcellulose (HPMC). Three distinct groups of maximum parameters, including polymeric solution, electrospinning method, and ambient parameter, are capable of influencing the creation along with the shape of those ultimate NFs. The prepared formulas of rosuvastatin calcium nanofibers (RC-NFs) were evaluated for nanofibers diameter, dissolution profiles, free standing microscopy with electrons and fourier transformation infrared (FTIR) spectroscopy are also available. As a consequence, the velocity of dissolution increases as the particle's surrounding area increases because of the its small size decrease to the nano level. The optimum ES parameters of polymeric solution (polymer type, concentration, combination, and effect of solvent type), ES process (injection flow rate, voltage, needle gauge, collector round per minute, needle to collector distance and collector type) and ambient parameter are tested and determined. Results show that four selected formulas of NFs are (F12, F14, F15 and F19) with an average diameter of (95, 120, 100 and 80 nm) respectively. The best ultrafine, smooth and beadless NFs is (F19) determined the fact that the narrower the circumference of the RC-NFs, the quicker its breakdown and the shorter the period of this medicinal component's liberation.

Keywords: Rosuvastatin calcium, Nanofibers, Rosuvastatin calcium nanofibers, Electrospinning, Polyethylene oxide, Polyvinyl pyrrolidone, Hydroxy propyl methyl cellulose.

International Journal of Drug Delivery Technology (2023); DOI: 10.25258/ijddt.13.4.22

How to cite this article: Mohammed IA, Al-Gawhari FJ. Formulation, Characterization, Optimization, and *In-vitro* Evaluation of Rosuvastatin as Nanofiber. International Journal of Drug Delivery Technology. 2023;13(4):1258-1266.

Source of support: Nil.

Conflict of interest: None

INTRODUCTION

Currently, more than 60% of drug molecules have poor water solubility and the new drug candidates have both high solubility and permeability represent only 8%. As a result the potentially important drugs are not achieving their full potential and do not marketed.¹ The drug's ability to dissolve in water is an aspect of restricting phase in its breakdown, and inadequate solubility results in an influential dissolving speed. Challenges usually result in reduced bioavailable of orally delivered medicines.²

Since the greatest concentration of medicine is liquid in fewer than 250 mL of water throughout a pH range of (1.0) to (7.5), the drug is called extremely liquid. Molecules with solubilities less than 0.1 mg/mL, on the other hand, encounter severe breakdown challenges, and even molecules with solubilities less than 10 mg/mL often encounter dissolution problems throughout preparation.³

The drug's bioavailability is mostly determined by nanoparticle size; as a single molecule grows lesser, its total

surface region to volume concentration decreases. This serves as a catalyst for more contact with the financially sound, which increases the rate of breakdown. Since micronized atoms tend to clump together, the follow-up stage is nanonization.⁴

Nanomaterials are defined by the US Food and Drug Administration (USFDA) as "materials with not less than one measurement in a frequency range of about 1 to 100 nm and show category sensitive activities."⁵ NFs, like nanorods and nanotubes, are geometrically classified as one-dimensional nanoscale components. Therefore, NFs have characteristic advantages such as high surface area, extremely porous structure and surface morphologies that make them suitable for drug development and offer solutions for drug solubility, dissolution, bioavailability and delivery obstacles.⁶ Many methods of preparation and fabrication of nanofibers including phase division, creating art, pattern manufacturing, liquid blown technologies, force Spinning, and electrospinning.⁷ Historically, the initial discovery of an ES method relies on

*Author for Correspondence: ehsan2013.mohamed@gmail.com

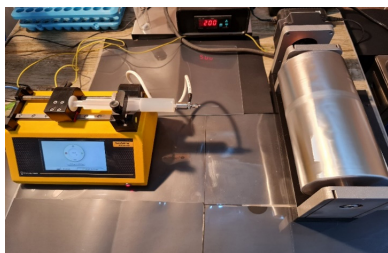


Figure 1: Electrospinning apparatus

Table 1: Composition of RC-NFs formulas

Formula	Rosuvastatin calcium %	PEO (300) *(10000)	PVP K30 (60000)	HPMC %
F1	1	0.3		
F2	1	0.5		
F3	1	0.7		
F4	1		8	
F5	1		12	
F6	1		16	
F7	1			1
F8	1			3
F9	1			5
F10	1	0.3	16	
F11	1	0.5	12	
F12	1	0.7	8	
F13	1	0.3		5
F14	1	0.5		3
F15	1	0.7		1
F16	1		8	5
F17	1		12	3
F18	1		16	1
F19	1	0.3	8	1
F20	1	0.5	12	3

an electromagnetic capability of extremely high voltage and extremely low flow for generating NFs by employing a solution of polymer or a melting state in 1902 by J. F. Cooley approach with the name of “Apparatus for electrically dispersing fibres” in 1902. The polymer was ejected through a syringe needle tip, and an elevated voltage was applied to create electric motion in the polymer fluid and extend the shape of the typically produced by the outer stress globe hanging fall into Taylor’s cones, and the flow beginning begins from the cones add one time the magnetic attraction effect exceeds the amount of surface tension. Essentially, the two pressures that cause Taylor’s cone to take shape are regulated implicitly by the voltage being applied and the velocity of flow. The entire procedure was followed by the evaporation of the solvent. NFs are collected over an alloy filter, that’s just a piece of foil made of aluminum mounted at an optimized needle-to-collector relationship.⁸

The goal of this work was to improve the disintegration and solubility characteristics of the group II insoluble in water anti-dyslipidemia medication RC by producing it as RC-NFs utilizing ES technique.

MATERIALS AND METHOD

Materials

RC powder was purchased from (AOpharm, China), polyethylene oxide (PEO) (Average molecular weight 300*10000), polyvinyl pyrrolidone (PVPK-30), and hydroxypropyl methylcellulose (HPMC) (HI Media Laboratories, India). Methanol (GCC Analytical reagent, UK) brij 35 (Polyoxyethylene (23) lauryl ether) (Riedal De Haen Ag Seelze, Hannover, Germany). Mannitol and magnesium stearate (Barlocher, GMBH, Germany).

Method

Preparation of RC-NFs

RC-NFs were prepared by using an electrospinning apparatus for NFs production from Inovenso electrospinning company -

Table 2: Variable parameters of RC-NFs formulas preparation.

Parameter	Flow rate (mL/h)	Voltage	Needle internal diameter	Speed of collector (rpm)	Solvent ratio Methanol: Water	Distance between needle and collector (cm)
1	1	15 KV.	G 23	200	50:50	12
2	0.5	15 KV.	G 23	200	50:50	12
3	2	15 KV.	G 23	200	50:50	12
4	1	10 KV.	G 23	200	50:50	12
5	1	20 KV.	G 23	200	50:50	12
6	1	15 KV.	G 21	200	50:50	12
7	1	15 KV.	G 19	200	50:50	12
8	1	15 KV.	G 23	400	50:50	12
9	1	15 KV.	G 23	100	50:50	12
10	1	15 KV.	G 23	200	40:60	12
11	1	15 KV.	G 23	200	60:40	12
12	1	15 KV.	G 23	200	50:50	8
13	1	15 KV.	G 23	200	50:50	16

a nanotechnology engineer in Istanbul, Turkey. A particular level of natural RC and polymer medicine was entirely absorbed in a methanol/water-soluble liquid.

The obtained drug polymeric solution was then injected using a syringe electrospinner into the drum collector as shown in Figure 1. Deposition of solid drug NFs occurred immediately upon solvent evaporation.

The composition of prepared 20 formulas and variable parameters of preparation tested from (1-13) for all 4 selected RC-NFs formulas (F12, F14, F15 and F19) are listed in Tables 1 and 2.

Evaluation of RC-NFs

Determination of RC content in NFs

To determine the drug concentration of the produced RC-NFs, a 100 mg sample of each created formulation was pulverized completely in a glass mortar with methanol. The whole mixture was poured into a flask with a volumetric cap after carefully cleaning all equipment, and the volume was completed to 100 mL with formaldehyde (96%). To achieve full RC disintegration, the resulting distribution had to be sonicated for 15 minutes. The combination was processed through conventional filter paper, and the spectroscopic absorbance of RC (max at 241 nm) was measured spectrophotometrically. The curve that serves as a calibration was used to determine the quantity of medication within the NFs.⁹

Determination of rosuvastatin calcium - nanofibers saturation solubility

The solvent solubility of the chosen drug called microfibers formulations was assessed by performing a steady-state dissolution assessment for RC solubility utilizing the shake flask technique for various test medium water, HCl pH 1.2, and a buffered phosphate buffer pH 6.8. An excess of the medication was added to 10 mL of solution in a sample bottle and agitated for 48 hours in an ice bath with the shakers at 25°C as shown in Table 3. The drug concentration of sifted materials was determined spectrophotometrically.¹⁰

Nanofibers surface morphology studies - scanning electron microscopy

The measurement of the diameter along with shape of the resulting fibers has been identified using an FEI Quanta 450 scanning electron microscope (Made in the Czech Republic by FEI American company) with different electron-beam acceleration voltage and different magnification values: the sample was placed on the sample holder using double-sided tape. Image J software (National Institutes of Health, Bethesda, MD, USA) was used to assess fiber sizes. The findings provided are predicated on observations from at least 100 fibers.¹¹

Preparation of RC-NFs Incorporated Tablets

The RC-NFs of the chosen formulations were correctly weighed and passed through 20 mesh sieves with all additives (excluding the lubricants) as specified in Figure 3. For 15 minutes, the granular material was combined. The blending process was extended for a period of time following the use of

Table 3: Composition of RC-NFs incorporated tablets

<i>Formula: RC polymeric nanofiber tablet</i>	<i>F19</i>
Rosuvastatin calcium - Nanofibers equivalent to	
Rosuvastatin calcium mg	10
Aspartame	6
Talc	2
Mg-stearate	2
Mannitol sufficient to	200 mg

a small amount of magnesium stearate as a lubrication. The finished combination was crushed at 5 KN pressurization force employing a 9 mm one-blow pill device.¹²

Fourier transform infrared spectroscopy

Bruker- FTIR was used to acquire the results of the fourier transform infrared spectroscopy (FTIR) spectrum. Pure a medication called PEO, PVP, HPMC, and RC-NFs from the chosen combination (F19) have been evaluated. The resulting spectra has a wave number range of 400 to 4000 cm⁻¹.¹³

In-vitro release study

The breakdown of the produced pills was studied. Regarding the in vitro dissolving tests, the USP paddles technique was employed. The dissolving media in this investigation was HCL liquid (pH 1.2) with 1% Brij 35 and the phosphate buffer solution (pH 6.8) with 1% Brij 35. The mixer’s speed was 75 2 rpm. All of the products included 10 mg of RC. The dose tablets were put in 900 mL of each medium and kept at 37 0.1°C. At appropriate time intervals (1, 2, 4, 6, 8, 10, 20, 30, 40, 50, and 60 minutes), Five mL of material were collected and processed with a 0.45 mm millipore filtering system. For the purpose of maintaining a consistent quantity, the dissolving fluid was changed with five mL of new breakdown fluid. All of the specimens were then examined by UV-spectrophotometer at the maximum concentration of rosuvastatin. The amount of medication released from each drug product was calculated using the average of all of three measurements.¹⁴

Statistical Analysis of Dissolution Data

Khan and Rhodes proposed the calculation of dissolution efficiency to evaluate the dissolution using the following equation.

$$DE = \frac{\int_{t_1}^{t_2} y \cdot dt}{y_{100} \times (t_2 - t_1)} \times 100 \tag{eq.1}$$

Here y is the disintegrated item proportion, DE is the measurement of the area underneath the evaporation curve among the two time points t1 and t2 represented as a percentage of the total of the peak graph breakup, y100, during exactly the same duration.

Moore and Flanner also used the equivalence parameter (f 2) to compare dissolving patterns using an alternative calculation..

$$f_2 = 50 \times \log \left\{ \left[1 + \frac{1}{n} \sum_{i=1}^n |R_i - T_i|^2 \right]^{-0.5} \times 100 \right\} \tag{eq. 2}$$

Here n is the all amount of disintegration periods and RT and Tt give the benchmark and test breakdown rates at moment t.¹⁵

RESULT AND DISCUSSION

Polymeric Solution Parameter

The influence of polymer type

The impact of several polymers on the mechanical characteristics of produced NFs was examined, including PEO (F1, F2, and F3), PVP (F4, F5, and F6), and HPMC (F7, F8, and F9). The outcomes of this aspect were documented, and Figure 2 revealed that PEO has greater spinnability homogeneous silky microfibers when compared to PVP and HPMC.

The influence of polymer composition

The impact of several polymer concentrations on anatomical characteristics of manufactured NFs was investigated: PEO (F1, F2, and F3), PVP (F4, F5, and F6), and HPMC (F7, F8, and F9). The findings of the NFs of the three polymers (PEO, PVP, and HPMC) presented in Figures 3, 4, and 5 suggest that increasing the quantity of polymer has an effect on RC-NFs average dimension. Raising polymer concentration increased mean microfibers dimensions, however only above polymer ideal levels was this seen.

The influence of the number of polymers on the solution's fluidity while it is small the connection of polymers that is required for fiber production fails to occur. When nanoparticles are produced, an effect known as applying electricity occurs.¹⁶

Since the solution's polymeric percentage is inadequate, the electrical field that is generated and contact tension lead the intertwined polymer chain links to disintegrate prior to getting to the point of collection, resulting in the creation of studded microfibers. Raising density leads to an upsurge in polymeric solution quantity, eventually promoting chains of polymer attachment, resulting in homogeneous beadless nanofibers made by electrospun by overcoming pressure on the surface. When the amount of polymers rises across the point of critical importance (polymer liquid with a percentage that results in ultrafine, homogeneous, fluid beadless NFs are created), the mixture of polymers dries at the needle tip, obstructing liquid movement. The ES mechanism is considerably altered by modifying the percentage of the polymeric remedy, which is dependent on the extending of a supercharged stream.¹⁷

Polymer mixture impact

A series of various plastics are additionally possible to achieve optimal NF characteristics, and in our studies, we found that using bi (F12, F14, and F15) and tri polymeric remedies (F19) increases the solution's polymer spinnability as well as generates eliminate identical beadless NFs with less extensive indicate lengths when compared to single polymeric remedies (F2, F5, and F8) Figure 6.¹⁸

Effect of solvent type and ratio

Water boiling point is 100°C with low intrinsic viscosity and upon electrospinning produces beaded and small diameter nanofibers when used alone. while in combination with methanol 64.7°C boiling point and high dielectric constant, small NFs diameter (F19) 80 nm are produced till 50% methanol concentration then increase fiber diameter with increase

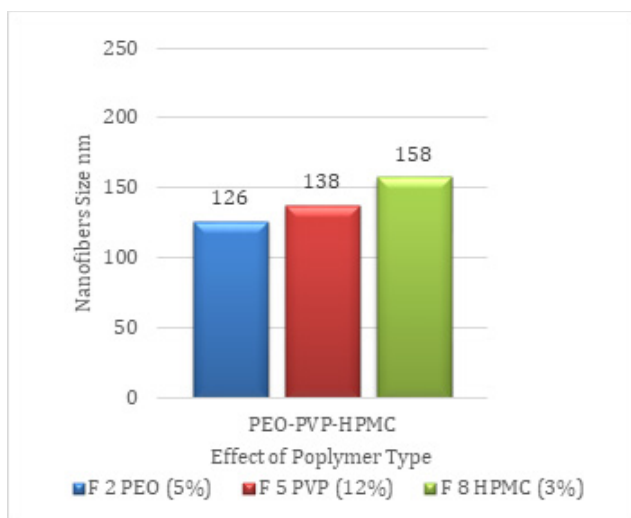


Figure 2: Effect of polymer type on nanofibers size in nm (p 0.003)

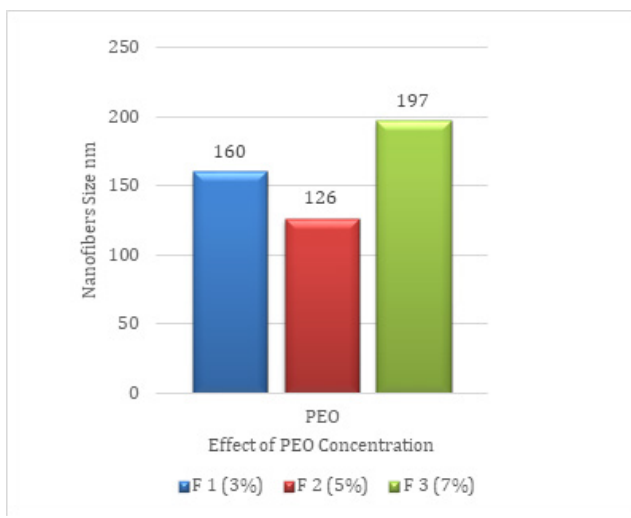


Figure 3: Effect of PEO concentration on nanofibers size in nm. (p 0.004)

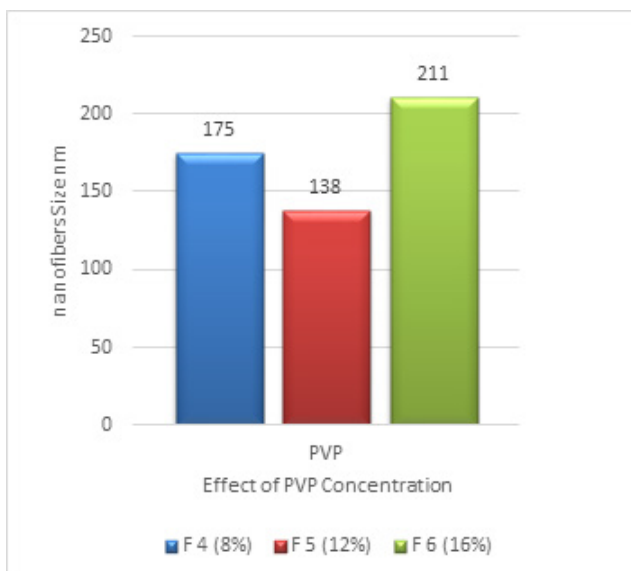


Figure 4: Effect of PVP concentration on nanofibers size in nm. (p 0.004)

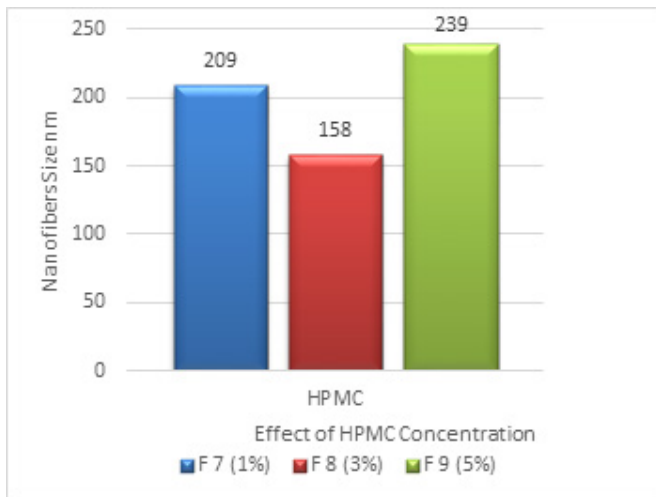


Figure 5: Effect of HPMC concentration on nanofibers size in nm. (p 0.004)

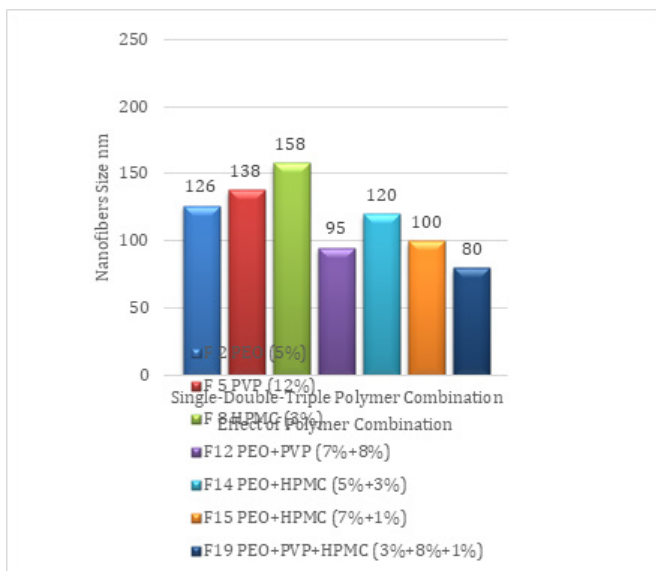


Figure 6: Effect of polymer combination on nanofibers size in nm. (p 0.002)

methanol concentration into 60% to result in 110 nm. While increasing water to 60 results in beaded nanofibers Figure 7.

The fluid’s point of vaporization and the dissolution of a certain polymer in this solution are two crucial elements to consider when selecting a chemical to create NFs *via* ES. The chemical solvent instability affects microfiber degradation throughout migration from the needle collection tip to the collection interface. Furthermore, extremely low simmering temperatures produce fast absorption at the instrument’s tip, blocking the mixture’s velocity of flow. Furthermore, liquids that have elevated boiling degrees may not totally dryness before arriving at their destination. which causes ribbon-like NFs shape or microfiber conglutination at the point of capture.^{19,20}

To affect the solution characteristics, shape, and diameter of NFs, several solvent-based systems with varied ratios are used. In addition to the printed NFs’ thermomechanical

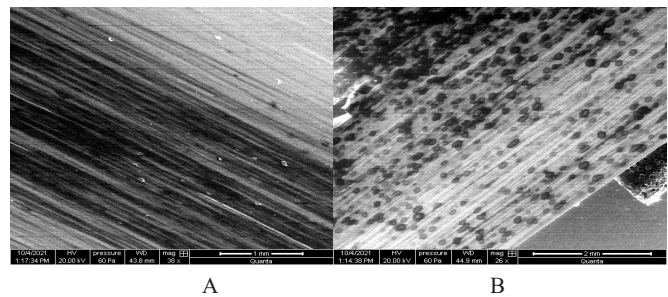


Figure 7: A. Methanol: Water – 50:50 and B. 40:60 Methanol: Water.

characteristics and breakdown dynamics.²¹ Separation of phases happens at the interface between the liquid and the air and determines the shape of the NFs formed as a consequence of fluid instability. To obtain the requisite seamless, identical, and beadless NFs, a favorable mix of co-borrowers with varying boiling temperatures is used.²²

ES Process Parameter

Effect of injected flow rate

The exchange frequency of the polymer mixtures from the point of the needle determines the form of the NFs. Because it affects the speed at which the polymer mixture is transmitted from the spinneret to the a gatherer.^{23,24} Consistently use a reduced flow speed to allow for polarization and evaporated solvent, permitting clean NFs coating on a gatherer.^{24,25} Applying high flow rates beaded NFs formed due to short drying time and low stretching forces for the NFs before deposition on the collector.^{24,26} In our work using a lower flow rate 0.5 mL/hr and a higher flow rate of 2 mL/hr comparison to 1-mL/hr have no significant effect on nanofibers diameters of selected formulas with resulting beaded nanofibers with increasing flow rate after 2 mL/hr.

Effect of voltage

In order to prevent the creation of droplets and electrospaying, the speed of flow as well as voltages are really adjusted collectively to achieve a steady Taylor cone structure.²⁷ While a small drop of a polymeric solution emerges on the tip of a metal-conductive needle and an intense voltage (5–50 kV) is provided, the resulting droplet becomes strongly illuminated, with the generated electrons evenly spread across its outer layer. The droplet will then compress into a “Taylor cone” shape.²⁸ While voltage being applied has an impact on NFs length, the magnitude of the impact depends on the polymer content of the solution and the instrument to the seller separation.²⁹

In the current investigation, microfibers with shorter diameters were generated using a small amount of the polymer mixture (F 19), needles to gatherer length (12 cm), and a voltage source of 10 kV.

Effect of needle gauge

In this study needle gauge 23 fabricated thinner and smoother nanofibers without bead formation or agglomeration compared with needles gauge 19 and 21, respectively. While flow

blockage with gauge 24 needle. These findings aided the development of electrostatic force, which is accountable for expanding and thinning the polymeric stream.

In theory, employing an extremely small needle length could end up in thinner and lesser length NFs due to the creation of a tiny amount with a substantial surface tension of polymeric solution contrasted to a big tip length. The greater the possibility distinction, the greater the magnetic attraction exerted to the polymeric drop, expanding and making the stream narrower.³⁰

Effect of round per minute

In our experiments, an elevated utilization rate of 400 rpm breaks the fibre aircraft and collects highly oriented and identical lengthy NFs at 200 rpm, whereas a greater quantity of corresponded fibres is fabricated due to leftovers buildup of charges on the placed NFs at 100 rpm, which crosses with the proper positioning of arriving fibres. The standard diameter of NFs reduces as the spinning gatherer rpm increases, however, the fall in frequency does not seem substantial in relation to other characteristics.

NFs might be orderedly matched by revolving a drum gatherer at thousands of rpm. While the rpm meets the formation of a vaporized jet, the fibers match on the drum collector's aluminum foil. This is referred to as a connection rate. If the container collector's rpm is less than the prescribed rapidly, fibers are gathered at arbitrarily. Finally, there has to be an ideal spinning rate beyond that consecutive fibers are unsuitable for collection.^{31,32}

Effect of needle-to-collector distance

In this study lower mean diameter values for all four selected formulas (F12, F14, F15 and F19) at optimal needle to drum collector distances of 12 cm. A farther away of 16 cm from the tip of the needle and the drum gatherer caused fibers to separate and be disposed of before reaching the part that collects them. Ring production is noticed at shorter lengths because the plastic jet lacks enough time to harden at 8 cm.

The separation between the point of the needle and drum gatherers controls the strength of the electromagnetic radiation and, therefore determines the form of the fiber. Less range needs less time for a solution being dried, and fibres hold together to produce more massive NFs, but farther away demands a greater KV For fiber production.³³

Effect of different types of collector

A fixed surface gatherer has a greater mean NFs size score than a drum that rotates gatherer. In this study mesh cross-linked nanofibers deposit on a plate while aligned fibers are obtained with rotary collector as shown in Figure 8.

A capacitive aluminum foil sheet serves as a gatherer in simple ES installations to generate a possible distinction between the point of the needle and the object being collected. When compared to plate collectors, revolving drum collectors aid in obtaining dry fibers since the fibers have a longer period for the evaporation of solvents. If the collector's collecting rate is less rapid than the critical percentage of orientation

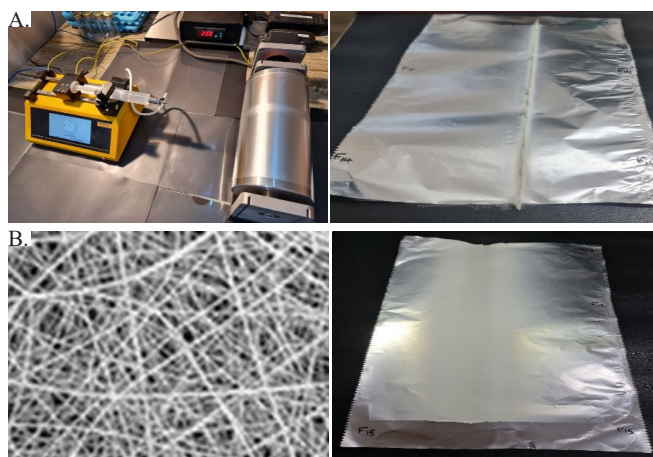


Figure 8: A. Drum collector fiber alignment in the center B. Plate collector mesh cross-linked nanofibers deposit.

Table 4: Solubility data of the RC and RC-NF (F19) selected formula in different media

Solvent	Solubility of RC (mg/mL)	Solubility of F19 (mg/mL)
Water	3.6	9
HCl Buffer pH 1.2	0.6	3.6
Phosphate Buffer pH 6.8	1	7

quickness, more fibres are gathered in the gatherer, where charge assembly may reject the arriving fiber, meaning lower-orientated fibres.³⁴

Effect of ambient parameter

Result of our work show that there is no significant difference in morphology and average diameter of NF reverse to what mentioned in references and studies when we change the experiment ambient parameter of temperature and humidity of (25°C/60) and (40°C/65).³⁵

NFs excessive solubility analysis of formulated NFs

in the ability to dissolve of the chosen compound F19 at various pH levels was found, as given in Figure 5. The maximum mobility of the suggested formula's RC-NFs in water, HCl pH 1.2, and Phosphorus Buffer pH 6.8 was raised by 1.5, 5, and 7 creases, respectively, when compared to a pure RC. The rise in maximal concentration of formula F19 is primarily attributed to the nanonization impact.^{36,37}

Surface morphology of nanofibers using scanning electron microscopy

The SEM pictures of the NFs derived from the specified equations (F19) displayed in Figure (9) show consistent, homogeneous nano-sized in-thickness fibers.

Fourier transformations using infrared spectroscopy for drug interaction

The fourier transform infrared spectrum provides a little understanding of the chemical structures that might collaborate with the additive throughout the preparation. The typical maximum can be seen in the infrared portion of RC Figure 10.

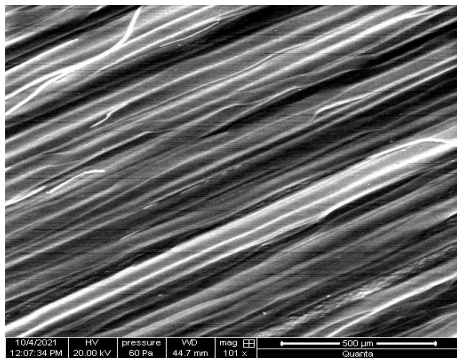


Figure 9: Scanning electron microscope image of F19 nanofibers

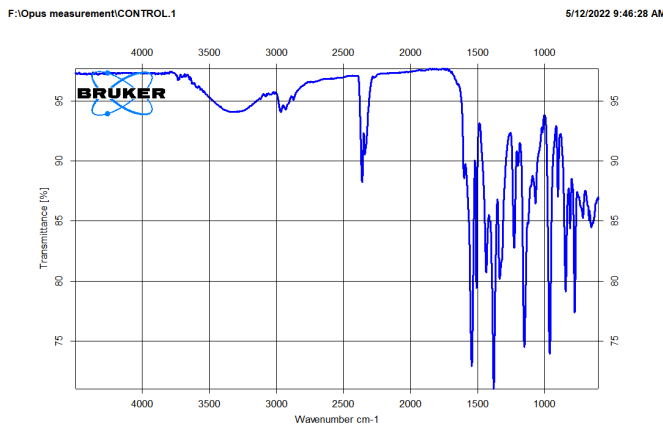


Figure 10: FTIR spectrum of pure rosuvastatin powder

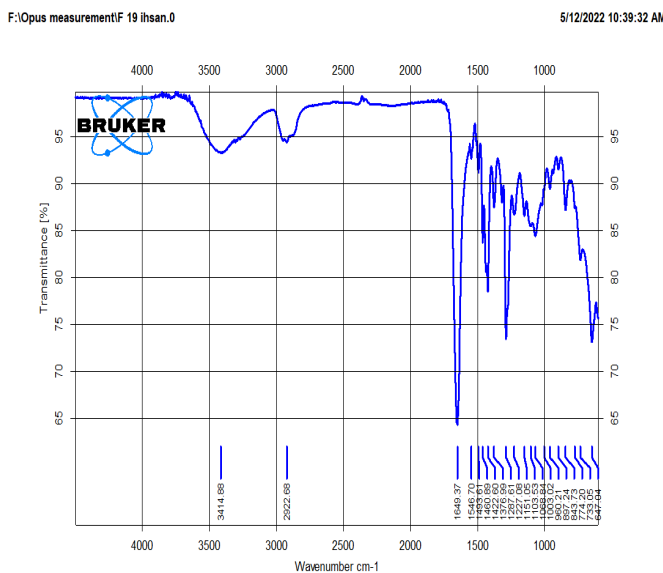


Figure 11: FTIR spectrum of F19 nanofibers

The spectra of the suggested formulations of RC-NFs (F19) shown in Figure 11 show an abundance of the medication's fundamental peak periods, indicating in there is no substantial connection between the medication and polymers throughout microfibers synthesis.

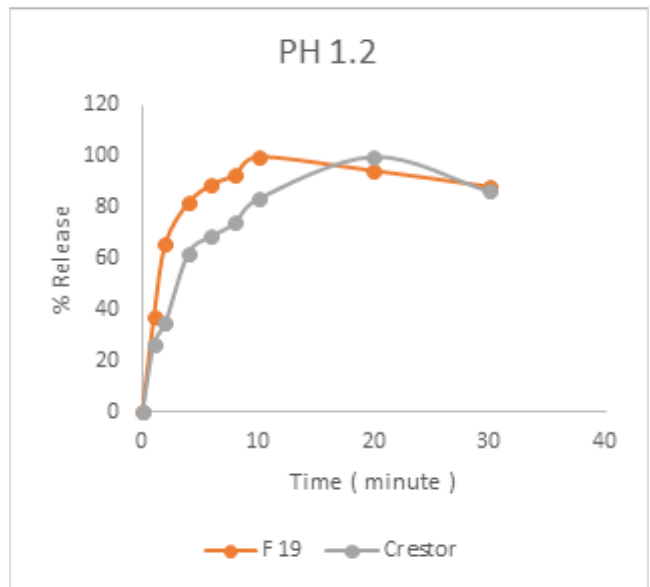


Figure 12: Dissolution profile of rosuvastatin nanofibers tablet F 19 and Crestor ® tablet in HCl pH 1.2 with 1% Brij

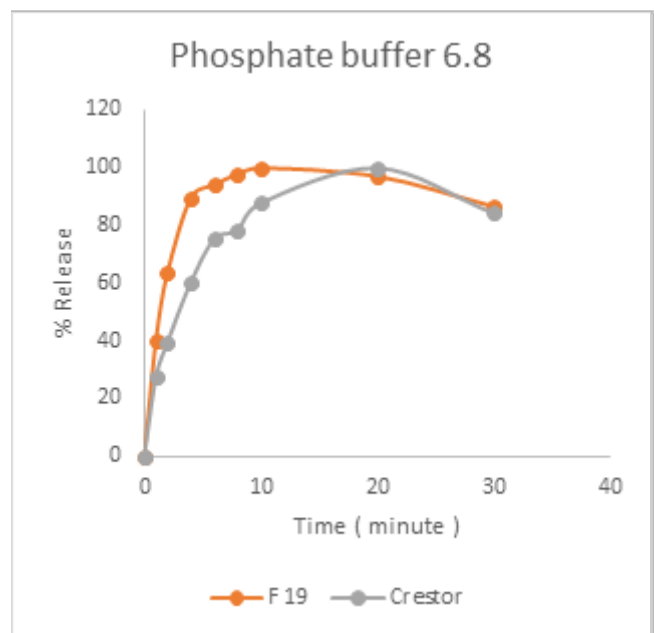


Figure 13: Dissolution profile of rosuvastatin nanofibers tablet F 19 and Crestor ® tablet in phosphate buffer pH 6.8 with 1% Brij 35.

In-vitro Release Study

The findings of a disintegration analysis of a commercially available tablet (Crestor®) at various medium pHs demonstrate variations with the RC-NFs formula in terms of disintegration effectiveness (DE) and consistency component (f₂). In both conditions, the pH was 1.2 in HCL (DE = 89%) and 6.8 in a buffered phosphate solution (DE = 91%). On the other hand, significant improvements in dissolving are reflected by the dissolve effectiveness of RC-NFs including pills of 92 and 95% for the F 19 displayed Figures (12 and 13), owing mostly

to nanosizing of the fragments, which improves fluidity. In accordance to the Noyes-Whitney formula, the degree of solid disintegration is inversely correlated to the exterior region contacted by the disintegration media.

The resemblance component f_2 measures the %solubility similarity among the two curves of marketed-reference medication and chosen preparation F19. According to the present FDA criteria, both identities are regarded as identical if f_2 is larger than 50 (50–100), which corresponds to an actual variation of 10% across all sample periods. For F19 nanofibers was increased the resemblance component is 86.

CONCLUSION

We can come to the following conclusions based on how our work turns out. Different polymers and polymer combinations with concentrations change. Significantly affect RC-NFs average diameter. PEO demonstrated higher spinnability, and consistent smooth nanofibers, compared to PVP and HPMC, among the three polymers employed. The average nanofiber diameter increased with increasing polymer concentration, but only above the polymer critical concentration. The use of polymer combinations increases solution spinnability and results in smooth, uniform, beadless NFs. Small NFs are formed up to 50% methanol concentration, and as the methanol concentration rises to 60%, fiber diameter increases. Beaded nanofibers are produced when the water ratio is increased to 60%. The optimum flow rate to produce uniform smooth nanofibers was 1 mL/hr. Applied voltage of 10 kV, NFs with a smaller diameter were created. Needle gauge 23 produces thinner and smoother nanofibers without bead formation or agglomeration. Collection of highly aligned and uniform long nanofibers at 200 rpm. Lower NFs diameter values at optimum distances of 12 cm between the needle and drum collector. The mean A permanent surface gatherer has a larger NFs circumference than a revolving drum a gatherer. In this study mesh cross-linked nanofibers deposit on plate while aligned fibers are obtained with the rotary collector. The saturation solubilities of RC-NFs selected formula F19 in water, pH 1.2 HCl solution and pH 6.8 Phosphate buffer were increased (1.5.5 and 7) folds respectively relative to a pure RC. *In-vitro* study results the dissolution efficiency of the RC- F19 shows increment to (DE = 92% and 95%) (pH 1.2 and pH 6.8) respectively, compared with commercially available drug (DE = 89 and 91%). Also, f_2 is 86 which approves a similar dissolution profile between curves. The FTIR spectra of the selected formulas F19 show no significant interaction during the formulation and production of nanofibers.

REFERENCES

- Mehta S, Joseph NM, Feleke F, Palani S. Improving solubility of BCS class II drugs using solid dispersion: a review. *J drug Deliv Ther.* 2014;4(3):7–13.
- Wilson V, Lou X, Osterling DJ, Stolarik DF, Jenkins G, Gao W, et al. Relationship between amorphous solid dispersion in vivo absorption and in vitro dissolution: phase behavior during dissolution, speciation, and membrane mass transport. *J Control Release.* 2018;292:172–82.
- Chavda H, Patel C, Anand I. Biopharmaceutics classification system. *Syst Rev Pharm.* 2010;1(1):62.
- Sunder S, Nair R. Methods of nanonization of drugs for enhancing their dissolution. *Eur J Adv Eng Tech.* 2016;3(8):101–10.
- Guidance D. Considering Whether an FDA-Regulated Product Involves the Application of Nanotechnology. FDA. 2011;
- Chen J, Zhang T, Hua W, Li P, Wang X. 3D Porous poly(lactic acid)/regenerated cellulose composite scaffolds based on electrospun nanofibers for biomineralization. *Colloids Surfaces A Physicochem Eng Asp [Internet].* 2020;585:124048. Available from: <https://doi.org/10.1016/j.colsurfa.2019.124048>
- Kharde Sagar N, Saravanan K. Nanofibers as a platform for drug delivery: A review. 2019;
- Luraghi A, Peri F, Moroni L. Electrospinning for drug delivery applications: A review. *J Control release.* 2021;334:463–84.
- Yousefi P, Dini G, Movahedi B, Vaezifar S, Mehdikhani M. Polycaprolactone/chitosan core/shell nanofibrous mat fabricated by electrospinning process as carrier for rosuvastatin drug. *Polym Bull.* 2021;1–19.
- Emad H, Abd-Alhammid SN. Improvement of the Solubility and Dissolution Characteristics of Risperidone via Nanosuspension Formulations. *Iraqi J Pharm Sci.* 2022;31(1):43–56.
- Vázquez-González Y, Prieto C, Stojanovic M, Torres CA V, Freitas F, Ragazzo-Sánchez JA, et al. Preparation and Characterization of Electrospun Polysaccharide FucoPol-Based Nanofiber Systems. *Nanomaterials.* 2022;12(3):498.
- Démuth B, Farkas A, Szabó B, Balogh A, Nagy B, Vágó E, et al. Development and tableting of directly compressible powder from electrospun nanofibrous amorphous solid dispersion. *Adv Powder Technol.* 2017;28(6):1554–63.
- Al Alwany AA. Echocardiographic Assessment of the Aortic Stenosis Valve Area: Parameters and Outcome. *Journal of Medicinal and Chemical Sciences.* 2022. 5(7): 1281-1288.
- Butt S, Hasan SMF, Hassan MM, Alkharfy KM, Neau SH. Directly compressed rosuvastatin calcium tablets that offer hydrotropic and micellar solubilization for improved dissolution rate and extent of drug release. *Saudi Pharm J.* 2019;27(5):619–28.
- Ghareeb MM, Mohammed IA. Investigation of Solubility Enhancement Approach of Ticagrelor. *Iraqi J Pharm Sci.* 2018;27(1).
- Ahmed FE, Lalia BS, Hashaikeh R. A review on electrospinning for membrane fabrication: Challenges and applications. *Desalination.* 2015;356:15–30.
- Haider A, Haider S, Kang I-K. A comprehensive review summarizing the effect of electrospinning parameters and potential applications of nanofibers in biomedical and biotechnology. *Arab J Chem.* 2018;11(8):1165–88.
- Huang W, Yang Y, Zhao B, Liang G, Liu S, Liu X-L, et al. Fast dissolving of ferulic acid via electrospun ternary amorphous composites produced by a coaxial process. *Pharmaceutics.* 2018;10(3):115.
- Al-Hazeem NZA. Nanofibers and electrospinning method. *Nov Nanomater Appl, Georg Kyzas, ed, InTechOpen.* 2018;191–210.
- Yu D-G, Li J-J, Williams GR, Zhao M. Electrospun amorphous solid dispersions of poorly water-soluble drugs: A review. *J Control release.* 2018;292:91–110.
- Xu Y, Zou L, Lu H, Kang T. Effect of different solvent systems on PHBV/PEO electrospun fibers. *RSC Adv.* 2017;7(7):4000–10.
- Pillay V, Dott C, Choonara YE, Tyagi C, Tomar L, Kumar P, et al. A review of the effect of processing variables on the fabrication

- of electrospun nanofibers for drug delivery applications. *J Nanomater.* 2013;2013.
23. Huan S, Liu G, Han G, Cheng W, Fu Z, Wu Q, et al. Effect of experimental parameters on morphological, mechanical and hydrophobic properties of electrospun polystyrene fibers. *Materials (Basel).* 2015;8(5):2718–34.
 24. Li Z, Wang C. Effects of working parameters on electrospinning. In: *One-dimensional nanostructures.* Springer; 2013. 15–28.
 25. Hegab H, Tariq M, Syed NA, Rizvi G, Pop-Iliev R. Towards analysis and optimization of electrospun PVP (polyvinylpyrrolidone) nanofibers. *Adv Polym Technol.* 2020;2020.
 26. Acik G, Cansoy CE, Kamaci M. Effect of flow rate on wetting and optical properties of electrospun poly (vinyl acetate) micro-fibers. *Colloid Polym Sci.* 2019;297(1):77–83.
 27. Fadil F, Affandi NDN, Misnon MI, Bonnia NN, Harun AM, Alam MK. Review on electrospun nanofiber-applied products. *Polymers (Basel).* 2021;13(13):2087.
 28. Torres-Martínez EJ, Cornejo Bravo JM, Serrano Medina A, Pérez González GL, Villarreal Gómez LJ. A summary of electrospun nanofibers as drug delivery system: drugs loaded and biopolymers used as matrices. *Curr Drug Deliv.* 2018;15(10):1360–74.
 29. Akhgari A, GHALAMBOR DA, Rezaei M, Kiarsi M, ABBASPOUR MR. The design and evaluation of a fast-dissolving drug delivery system for loratadine using the electrospinning method. 2016;
 30. Supaphol P, Chuangchote S. On the electrospinning of poly (vinyl alcohol) nanofiber mats: a revisit. *J Appl Polym Sci.* 2008;108(2):969–78.
 31. Fajri RN, Sudarmaji A, Taqwa MZ. Design and Calibration of Drum Collector and ADC of High Voltage for Nanofiber Electrospinning based on Microcontroller Systems. In: *2020 10th Electrical Power, Electronics, Communications, Controls and Informatics Seminar (EECCIS).* IEEE; 2020. 163–7.
 32. Li N, Xiong J, Xue H. Effect of wheel rotating speed and LiCl additives on electrospun aligned polyacrylonitrile nanofiber. *Polym Eng Sci.* 2011;51(11):2178–83.
 33. Ahmadian A, Shafiee A, Aliahmad N, Agarwal M. Overview of nano-fiber mats fabrication via electrospinning and morphology analysis. *Textiles.* 2021;1(2):206–26.
 34. Islam MS, Ang BC, Andriyana A, Afifi AM. A review on fabrication of nanofibers via electrospinning and their applications. *SN Appl Sci.* 2019;1(10):1–16.
 35. Cuahuizo-Huitzil G, Santacruz C, Santacruzvaquez V. A review on electrospinning technologies and their potential use in the Biomedical Industry Capítulo 8 Una revisión sobre las tecnologías de electrohilado y su uso potencial en la Industria Biomédica. *Eng Technol.* :112.
 36. Rajput P, Gauniya A. Preformulation Studies of Rosuvastatin. *J Drug Deliv Ther.* 2019;9(3-s):729–35.
 37. Sharma A, Jain AP, Arora S. Formulation and In-Vitro evaluation of Nanocrystal formulation of poorly soluble drugs. *J Drug Deliv Ther.* 2019;9(4-s):1183–90.